# Three Regions within ActA Promote Arp2/3 Complex-mediated Actin Nucleation and *Listeria monocytogenes* Motility

**Justin Skoble,*  Daniel A. Portnoy,*‡ and Matthew D. Welch***

*Department of Molecular and Cell Biology, ‡School of Public Health, University of California, Berkeley, Berkeley, California 94720-3200

*Abstract.* The *Listeria monocytogenes* ActA protein induces actin-based motility by enhancing the actin nucleating activity of the host Arp2/3 complex. Using systematic truncation analysis, we identified a 136-residue $NH_2$-terminal fragment that was fully active in stimulating nucleation in vitro. Further deletion analysis demonstrated that this fragment contains three regions, which are important for nucleation and share functional and/or limited sequence similarity with host WASP family proteins: an acidic stretch, an actin monomer–binding region, and a cofilin homology sequence. To determine the contribution of each region to actin-based motility, we compared the biochemical activities of ActA derivatives with the phenotypes of corresponding mutant bacteria in cells. The acidic stretch functions to increase the efficiency of actin nucleation, the rate and frequency of motility, and the effectiveness of cell–cell spread. The monomer-binding region is required for actin nucleation in vitro, but not for actin polymerization or motility in infected cells, suggesting that redundant mechanisms may exist to recruit monomer in host cytosol. The cofilin homology sequence is critical for stimulating actin nucleation with the Arp2/3 complex in vitro, and is essential for actin polymerization and motility in cells. These data demonstrate that each region contributes to actin-based motility, and that the cofilin homology sequence plays a principal role in activation of the Arp2/3 complex, and is an essential determinant of *L. monocytogenes* pathogenesis.

Key words:   bacteria • pathogenesis • cell movement • cytoskeleton • microfilament proteins

## Introduction

The bacterial pathogen *Listeria monocytogenes* enters mammalian cells and escapes from the phagosome into the host cytosol, where it proliferates rapidly. In the host cytosol, *L. monocytogenes* induces the polymerization of actin filaments at its surface and initiates motility, generating comet tails of actin filaments and actin binding proteins that trail the moving bacteria (for review see Ireton and Cossart, 1997). The propulsive force for intracellular motility is derived from actin filament elongation at the interface between the bacterium and the actin tail (Mogilner and Oster, 1996), which remains fixed in place (Sanger et al., 1992; Theriot et al., 1992). Moving bacteria encounter the host plasma membrane and form filopod-like protrusions that are engulfed by neighboring cells (Tilney and Portnoy, 1989). Actin-based motility is essential for *L. monocytogenes* pathogenesis (Domann et al., 1992; Kocks et al.,

1992; Brundage et al., 1993), and has been studied as a model for understanding the regulation of actin dynamics in eukaryotic cells.

The bacterial cell surface protein ActA is necessary and sufficient for actin-based motility in host cytosol (Domann et al., 1992; Kocks et al., 1992; Pistor et al., 1994; Smith et al., 1995; Cameron et al., 1999). ActA can be divided into three domains that have distinct functions. The COOH-terminal domain (amino acids 391–639) contains a transmembrane sequence that is essential for anchoring ActA to the bacterial surface. The central domain (amino acids 264–390) contains four proline-rich repeats that bind to Enabled/vasodilator-stimulated phosphoprotein (Ena/VASP) family proteins (Chakraborty et al., 1995; Gertler et al., 1996; Smith et al., 1996), which in turn bind to actin filaments (Reinhard et al., 1992; Bachmann et al., 1999) and the actin-binding protein profilin (Reinhard et al., 1995). The central domain is not required for actin-based motility, but contributes to the rate of movement and the percentage of moving bacteria (Lasa et al., 1995; Pistor et al., 1995; Smith et al., 1996). In contrast, the mature $NH_2$-terminal domain (amino acids 30–263) is essential for actin polymerization

in host cytosol (Lasa et al., 1995; Pistor et al., 1995), and can be sufficient for motility if artificially attached to the bacterial membrane (Lasa et al., 1997). However, the NH₂-terminal domain does not directly stimulate actin polymerization (Welch et al., 1998).

Actin nucleation at the surface of *L. monocytogenes* is mediated by the NH$_2$-terminal domain of ActA together with the Arp2/3 complex (Welch et al., 1997, 1998), an evolutionarily conserved host protein complex consisting of the actin-related proteins, (Arp)[1], Arp2 and Arp3, and five other subunits (for review see Machesky and Gould, 1999). The Arp2/3 complex is required for bacterial actin-based motility in cell-free extracts (Egile et al., 1999; May et al., 1999; Yarar et al., 1999) and for reconstitution of actin-based motility from purified cytoskeletal proteins (Loisel et al., 1999). Three biochemical activities have been assigned to the Arp2/3 complex: pointed-end capping of actin filaments; cross-linking filaments into branched arrays; and weak nucleating activity thought to occur by stabilization of actin dimers (Mullins et al., 1997, 1998). In vitro, the nucleating activity of the Arp2/3 complex is dramatically stimulated by full-length ActA and by a truncated derivative consisting only of the mature NH$_2$-terminal domain (Welch et al., 1998). However, the regions within ActA that stimulate the Arp2/3 complex and the contribution of this interaction to motility and pathogenesis, have not been addressed.

In this study, we used deletion and truncation mutations in ActA to define the minimal fragment that nucleates actin polymerization with the Arp2/3 complex and to identify the functional elements within this fragment that contribute to nucleation in vitro and actin-based motility in infected cells. We identified three important regions, each of which shares limited sequence similarity or functional similarity with the Wiscott-Aldrich Syndrome protein (WASP) family of proteins, which has emerged as candidates for mediating actin polymerization at cell membranes by stimulating Arp2/3 complex nucleation activity (for reviews see Machesky and Insall, 1999; Welch, 1999). By comparing the activities of mutant ActA proteins in vitro with their corresponding phenotypes in cells, we have correlated the biochemical function of each region with its role in actin-based motility.

## Materials and Methods

### Generation of Mutations in the actA Gene

Plasmids encoding full-length 6xHis-tagged ActA and the derivative truncated at amino acid 263 were described previously (Welch et al., 1998). Additional truncations in *actA* were generated by PCR using VENT DNA polymerase (New England Biolabs) and the wild-type *L. monocytogenes* strain 10403S chromosomal DNA as a template. Primer CGGGATCCT-GAAGCTTGGGAAGCAG (DP-1717; BamHI site underlined) anneals upstream of the *ActA* promoter, and was used in combination with the downstream primer GCTCTAGATTAGTGATGGTGATGGTGATG-CCCGGGTCCCGTATTTACCTCGCT (XbaI and XmaI sites under-

lined) to amplify a DNA fragment that encodes the first 59 codons of *actA*, followed by a 6xHis tag. The BamHI-XbaI fragment was ligated into the gram−/gram+ shuttle vector pAM401 (Wirth et al., 1986) to yield plasmid pDP-3936. Each subsequent truncated derivative (truncated at amino acids 201, 165, 135, and 101) was generated by PCR using primer DP-1717 with primers listed in Table I (XmaI sites underlined). PCR products were digested with XbaI and XmaI, and subcloned into pDP-3936. For each construct, the DNA sequence of the insert was verified.

In-frame deletions in *actA* were generated using "splicing by overlap extension PCR" (Horton et al., 1990) as described previously (Smith et al., 1996). For each deletion, two primers were generated that were reverse compliments of one another and encoded bases flanking the region to be deleted. The forward primers are listed in Table I. Fragments upstream and downstream of the region to be deleted were amplified, and each pair of purified fragments was spliced in a third reaction. To generate 6xHis-tagged deletion derivatives, spliced fragments were cloned into pDP-2717, which contains the full-length His-tagged ActA (Welch et al., 1998).

### Allelic Exchange of In-frame ActA Deletions

To replace the 6xHis copy of *actA* on the 10403S chromosome with deletion alleles, DNA fragments were subcloned into temperature-sensitive vectors pKSV7 (Smith and Youngman, 1992), pCON1 (Moors et al., 1999), or pDP-3934 (a derivative of pKSV7 that contains a fragment of *L. monocytogenes* chromosomal DNA). The resulting plasmids were transformed into 10403S and allelic exchange was performed as described previously (Camilli et al., 1993), yielding strains listed in Table I. This strategy allowed the generation of isogenic strains of *L. monocytogenes* in which each allele was present in a single copy on the chromosome, maintaining all upstream regulatory elements as well as the endogenous transmembrane domain.

To verify that each strain contained the desired deletion, chromosomal DNA was amplified by PCR and the region flanking each deletion was sequenced. To confirm that the desired allele of *actA* was expressed on the surface of *L. monocytogenes*, bacteria were grown to mid-log phase in LB medium, washed with PBS, and the surface proteins were extracted by boiling in SDS-PAGE sample buffer as described previously (Brundage et al., 1993; Mourran et al., 1997). This treatment does not perturb the cell wall of *L. monocytogenes* and, thus, proteins in the bacterial cytosol are not released. Extracted proteins from cultures with equivalent cell densities (measured by taking the OD at 600 nm) were separated on a 7% SDS-PAGE gel and transferred to Immobilon-P membranes (Millipore). ActA was detected by immunoblotting using rabbit polyclonal antisera (DP-3997) raised against full-length His-tagged ActA.

### Expression and Purification of 6xHis-tagged ActA Derivatives

To eliminate the possibility that purified ActA derivatives were contaminated with endogenous ActA, an expression strain of *L. monocytogenes* was generated in which the entire chromosomal *actA* gene was deleted. This strain was produced by transforming *L. monocytogenes* strain DP-L1545 with a vector encoding a derivative of ActA with amino acids 7–633 deleted (pDP-3076) and performing allelic exchange as described above, yielding strain DP-L3935. The parent strain DP-L1545 is an *mpl*− derivative of SLCC-5764 (a strain that constitutively expresses high levels of ActA), which does not secrete the *prfA*-regulated metalloprotease that can degrade expressed ActA (Robbins et al., 1999). DP-L3935 was used to express high levels of ActA derivatives.

To isolate 6xHis-tagged ActA derivatives, plasmids encoding these proteins were transformed into DP-L3935, and secreted ActA derivatives were purified using procedures adapted from Welch et al. (1998). ActA deletion derivatives were precipitated from culture supernatant by adding ammonium sulfate to 400 g/liter (∼60% saturation). The precipitate was resuspended in wash buffer (20 mM Tris, pH 8.0, 250 mM NaCl, 20 mM imidazole, pH 7.0) and bound to 0.5 ml of Ni-NTA agarose (QIAGEN) per liter equivalent. The resin was washed 10 times with wash buffer and eluted with three bead volumes of wash buffer supplemented with 1 M imidazole, pH 7.0. Eluted proteins were desalted by passing two times over a G-25 (Amersham Pharmacia Biotech) spin column equilibrated in 2 mM Tris, pH 7.6, 0.2 mM CaCl and concentrated using microcon concentrators (Millipore). Protein concentrations were determined in triplicate by the BCA assay (Pierce) using BSA as a standard.

The truncated derivatives of ActA were not precipitated by ammonium sulfate, but were purified from culture supernatants by an alternative

---

[1]*Abbreviations used in this paper:* Arp, actin-related protein; F-actin, filamentous actin; G-actin monomeric actin; LB, Luria-Bertani; N-WASP, neuronal WASP; PtK2 *Potoroo tridactylis* kidney epithelial; VASP, vasodilator-stimulated phosphoprotein; WASP, Wiscott-Aldrich syndrome protein.

*Table I. Primers and Strains Used in this Study*

| ActA construct | Primer | 6xHis-tagged secreting strain | 10403S isogenic mutant strain |
|---|---|---|---|
| ActA | (Welch et al., 1998) | DP-L2723 | – |
| A263 | (Welch et al., 1998) | DP-L4007 | – |
| A201 | 5′-ATGCCCGGGTGTAGACTCGTCTGCTGA-3′ | DP-L3939 | – |
| A165 | 5′-ATGCCCGGGATAAGTAAGGCTTTCAAG-3′ | DP-L3942 | – |
| A135 | 5′-ATGCCCGGGATGACGACGCTCCACTTG-3′ | DP-L3944 | – |
| A101 | 5′-ATGCCCGGGACCTTTCTCTGCTTTTGC-3' | DP-L3946 | – |
| Δ31-262 | 5′-CCCGACATAATATTTGCAGCTAGCGACTTCCCGCCACCACCTACGGAT-3′ | DP-L3966 | – |
| Δ31-165 | 5′-CCCGACATAATATTTGCAGCGGATAAACCAACAAAAGCAAAT-3′ | DP-L3968 | DP-L3984 |
| Δ202-263 | 5′-TCAGCAGACGAGTCTACACCAGACTTCCCGCCACCACCTACG-3′ | DP-L3964 | DP-L3982 |
| Δ136-200 | 5′-CAAGTGGAGCGTCGTCATCCACCACAACCTTTAAAAGCAAATC-3′ | DP-L3972 | DP-L3988 |
| Δ60-165 | 5′-AGCGAGGTAAATACGGGACCAGATAAACCAACAAAAGCAAATAAG-3′ | DP-L3970 | DP-L3986 |
| Δ136-165 | 5′-CAAGTGGAGCGTCGTCATCCAGATAAACCAACAAAAGCAAAT-3′ | DP-L3974 | DP-L3990 |
| Δ146-150 | 5′-TCGGATAGCGCAGCGGAAATTGCCATAGCGTCGTCGGATAGT-3′ | DP-L3976 | DP-L3992 |
| Δ60-101 | 5′-AGCGAGGTAAATACGGGACCAAATAACAATAATAACAACGGTGAG-3′ | DP-L3978 | DP-L3994 |
| Δ31-58 | 5′-CCCGACATAATATTTGCAGCGCCAAGATACGAAACTGCACGT-3′ | DP-L3980 | DP-L3996 |
| Δ7-633 | 5′-ATTTTTTCTTAATTGAAATCTATTTAATCC-3′ | | DP-L3078 |

method adapted from Cameron et al. (1999). Overnight cultures were diluted 1:100 into modified D10 media supplemented with 10 μg/ml chloramphenicol and incubated for ∼12 h at 37°C with shaking. Secreted proteins were bound to Q-Sepharose fast flow resin (Amersham Pharmacia Biotech) and eluted with 20 mM Tris, pH 8.0, 1 M NaCl. Proteins in the eluate were bound to NiNTA agarose beads and purified as described above.

## Pyrene-Actin Polymerization Assays

Human platelet Arp2/3 complex (Welch and Mitchison, 1998), rabbit skeletal muscle actin (Spudich and Watt, 1971), and pyrene-labeled actin (Kouyama and Mihashi, 1981) were prepared as described previously. Pyrene-actin polymerization assays were performed as described previously (Cooper et al., 1983) with the following modifications. Pyrene-actin and unlabeled actin were mixed in G-buffer (2 mM Tris, pH 7.6, 0.2 mM CaCl, 0.2 mM ATP, 0.2 mM DTT) to generate a 4-μM monomer (G-actin) solution with <20% pyrene-actin. 6 μl of 200 nM Arp2/3 complex or 6 μl of control buffer (20 mM MOPS, pH 7.0, 100 mM KCl, 2 mM MgCl₂, 5 mM EGTA, 1 mM EDTA, 0.2 mM ATP, 0.5 mM DTT 10% vol/vol glycerol) was mixed with 6 μl 10× initiation buffer (20 mM MgCl₂, 10 mM EGTA, 5 mM ATP) and 18 μl G-buffer or up to 18 μl ActA in G-buffer. This 30-μl solution was mixed with 30 μl of G-actin solution to initiate polymerization. Assembly kinetics were monitored using a Fluorolog 3 fluorometer (Instruments S.A.; excitation wavelength 365 nm, emission wavelength 407 nm) maintained at a temperature of 25°C. The maximal rate of polymerization was determined by calculating the linear regression of the maximal slope using Kaleidagraph software (Synergy Software). Fold stimulation of polymerization by ActA was calculated by dividing the maximal rate of polymerization in the presence of ActA and Arp2/3 complex by the rate of polymerization in the presence of Arp2/3 complex alone. Fold inhibition of polymerization by ActA was calculated by dividing the maximal rate of polymerization in the absence of ActA by the maximal rate in the presence of ActA.

## Actin Pelleting Assay

Polymerization of 1 μM G-actin in the presence or absence of 5 μM ActA derivatives was initiated under the conditions described above. Polymerization was allowed to proceed for 10 min at room temperature, and F-actin was pelleted by centrifugation at 313,000 *g* for 10 min at 4°C. The supernatant was removed and the pellet was suspended in SDS-PAGE sample buffer. Approximately 1/2 of the total pellet fraction and 1/4 of the supernatant fraction were resolved on a 14% SDS-PAGE gel and protein was detected by staining with Coomassie blue.

## Immunoprecipitation of the Arp2/3 Complex and ActA

Polyclonal anti-p41 antibody (Yarar et al., 1999) and anti-goat IgG (Jackson ImmunoResearch Laboratories, Inc.) were covalently coupled to Affiprep protein-A support (Bio-Rad Laboratories) by incubation with 20 mM dimethyl pimelimidate (Pierce Chemical Co.). To generate Arp2/3 complex–coated beads, anti-p41 beads were incubated for 30 min at 4°C in human platelet extract that was preincubated with IgG-coated beads for 10 min at 4°C. Platelet extract was prepared by sonicating platelets in high salt sonication buffer (20 mM Tris, pH 8.0, 5 mM EGTA, 1 mM EDTA, 600 mM KCl, 0.1 μg/ml microcystin; Calbiochem), LPC (10 μg/ml leupeptin, pepstatin A, and chymostatin; Chemicon International), followed by centrifugation at 96,000 *g* for 10 min at 4°C. After incubation in the extract, beads were washed three times with high salt sonication buffer and three times with CoIP buffer (20 mM Hepes, pH 7, 100 mM KCl, 2 mM MgCl₂, 5 mM EGTA, 1 mM EDTA, 0.5 mM DTT, 0.2 mM ATP, 10% vol/vol glycerol, 2 mg/ml BSA and LPC). These high salt–washed Arp2/3 complex–coated beads were not contaminated by Arp2/3 binding proteins, as determined by SDS-PAGE and silver staining, nor were they contaminated with the ActA binding proteins actin or VASP, as determined by immunoblotting (data not shown). For ActA binding experiments, 50 μl IgG and Arp2/3-coated beads were incubated with 5 μl of 15-μM ActA derivatives and 100 μl CoIP buffer at room temperature for 30 min. The pellets were washed five times with 50 μl CoIP buffer lacking BSA. Bound proteins were eluted from the beads by the addition of SDS sample buffer, resolved on a 7% SDS-PAGE gel, and were transferred to nitrocellulose membranes; ActA was detected by immunoblotting using a rabbit polyclonal antisera (DP-3997).

## Analysis of L. monocytogenes–infected Tissue Culture Cells

HeLa and *Potoroo tridactylis* kidney epithelia (PtK2) cells were grown on glass coverslips in RPMI 1640 medium (Life Technologies) supplemented with 10% FBS, 2 mM glutamine and 1 mM pyruvate. Subconfluent monolayers were infected with *L. monocytogenes* as described previously (Smith et al., 1996). For fluorescence staining, HeLa cells were fixed with 3.2% paraformaldehyde at 3.5 h after infection. F-actin was stained with rhodamine-labeled phalloidin (Molecular Probes). VASP was detected with an affinity-purified rabbit polyclonal anti-VASP primary antibody (Smith et al., 1996), followed by an FITC-conjugated donkey anti–rabbit secondary antibody (Jackson ImmunoResearch Laboratories, Inc.). Host and bacterial DNA were stained with DAPI (4,6-diamidino-2-phenylindole). For quantification of bacteria associated with F-actin, infected PtK2 cells were fixed as above and stained with rhodamine-phalloidin and a rabbit polyclonal anti-*Listeria* antibody (DIFCO Laboratories), followed by an FITC-conjugated donkey anti–rabbit secondary antibody. Infected cells were visualized using a TE300 inverted microscope (Nikon). Images were captured with a CCD camera (Hamamatsu), pseudocolored, and were merged using Phase 3 imaging systems software.
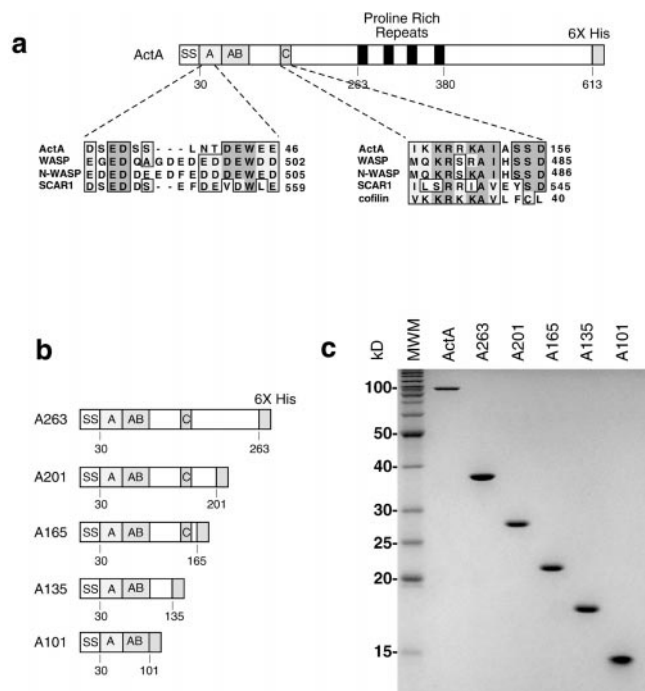
Motility rates were determined in infected PtK2 cells. At 3 h after infection, coverslips were transferred to a heated chamber and maintained in F-12 media (Life Technologies) with 5% FBS and 20 mM Hepes pH 7.0. Phase-contrast images were captured every 10 s for 5 min, and the rate of movement was calculated using Phase 3 imaging systems software.

Measurements were terminated if the bacteria stopped moving or encountered the plasma membrane. Plaque assays were performed in monolayers of L2 fibroblast cells as described previously (Sun et al., 1990; Jones and Portnoy, 1994). Plaque size was determined by capturing images using a digital camera and measuring the diameter of at least 15 plaques per experiment using Canvas (Deneba Software). Mutant plaque size was compared with wild type for each experiment.

## Results

### A 136–Amino Acid NH$_2$-terminal Fragment of ActA Is Sufficient to Stimulate Arp2/3 Complex Nucleating Activity
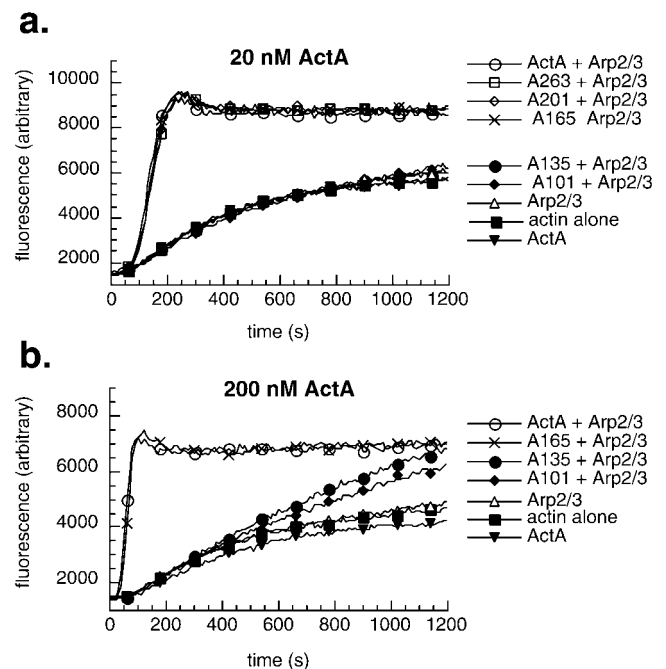
To define the regions within the NH$_2$-terminal domain of ActA that contribute to nucleation, we generated a series of 6xHis-tagged ActA derivatives that were truncated at amino acids 201, 165, 135, and 101 (A201, A165, A135, and A101, respectively; Fig. 1 b). Each was truncated at a proline residue, where the secondary structure was predicted to be a turn (Chou and Fasman, 1974), increasing the likelihood that the native secondary structure was preserved in the truncated molecules. Truncated ActA derivatives were expressed and purified (Fig. 1 c), and the capacity of each derivative to stimulate the nucleating activity of the Arp2/3 complex was measured using the pyrene-actin po-

lymerization assay (Kouyama and Mihashi, 1981; Cooper et al., 1983). As previously reported (Welch et al., 1998), equimolar concentrations of full-length ActA and Arp2/3 complex acted synergistically to accelerate actin nucleation, whereas ActA or Arp2/3 complex alone at this concentration had a negligible effect on polymerization kinetics (Fig. 2 a). The ActA derivatives A263, A201, and A165 were as potent as the full-length protein in their ability to stimulate polymerization with the Arp2/3 complex. In contrast, A135 and A101 had virtually no stimulatory effect. This suggests that the region between amino acids 135 and 165, which contains a cofilin homology sequence similar to that found in WASP family proteins (Fig. 1 a; Bi and Zigmond, 1999), is critical for actin nucleating activity.

These derivatives were also tested for their ability to stimulate nucleation when present at a 10-fold molar excess relative to the Arp2/3 complex. As was observed at lower concentrations, A165 and full-length ActA were equivalent in stimulating nucleation (Fig. 2 b). A135 and A101 stimulated nucleation to a greater extent than they had at lower concentrations, but were less potent than A165 (Fig. 2 b). By plotting the fold stimulation of the maximum rate of polymerization versus the concentration of full-length ActA or A101 (see Fig. 5), we were able to quantitatively compare the relative activities of these polypeptides. Whereas full-length ActA stimulated polymerization up to 25-fold at 10 times the concentration of Arp2/3 complex (see Fig. 5), A101 caused only a 3-fold stimulation at concentrations up to 100 times that of Arp2/3.
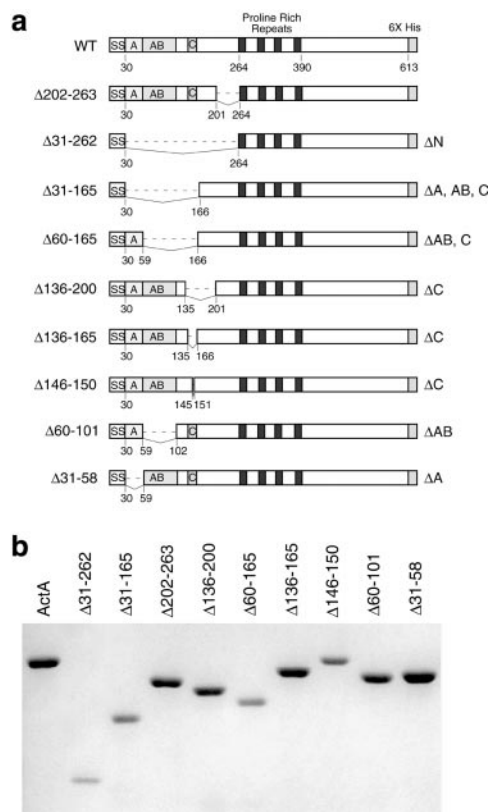


*Figure 1.* COOH-terminal ActA truncations. (a) Schematic diagram of secreted 6xHis-tagged ActA and sequence alignments with WASP family proteins and cofilin. The signal sequence is labeled SS. Regions within the mature NH$_2$ terminus are labeled as follows: acidic (A), actin binding (AB), and cofilin homology (C). The proline-rich repeats are shaded black, and the 6xHis tag is shaded in gray. (b) Diagram of derivatives of ActA that were truncated at amino acids 263 (A263), 201 (A201), 165 (A165), 135 (A135), and 101 (A101). (c) Purified-truncated derivatives of ActA visualized on a 15% polyacrylamide gel stained with Coomassie blue. The leftmost lane contains molecular weight markers (MWM).



*Figure 2.* Effects of truncated derivatives of ActA and Arp2/3 complex on actin polymerization kinetics. (a and b) Graphs of fluorescence intensity versus time after initiating actin polymerization in the pyrene-actin polymerization assay. (a) 2 μM actin in the presence or absence of 20 nM Arp2/3 complex and 20 nM ActA derivatives. (b) 2 μM actin in the presence or absence of 20 nM Arp2/3 complex and 200 nM ActA derivatives.

ActA is predicted to have a turn at proline 59 (Chou and Fasman, 1974), which may separate A101 into two distinct regions. One region (amino acids 30–59) contains a high proportion of acidic residues (11/28 are glutamate or aspartate) that share sequence similarity with the acidic stretch in WASP family proteins (Fig. 1 a). The other (amino acids 59–101) has been previously reported to have actin monomer–binding activity (Lasa et al., 1997; Cicchetti et al., 1999). The above findings indicate that these two regions alone retain some stimulatory capacity, suggesting that they contribute to nucleation in the context of the full-length protein.

### Three Regions within the NH₂-terminal Domain of ActA Have Distinct Functions in Actin Nucleation with the Arp2/3 Complex
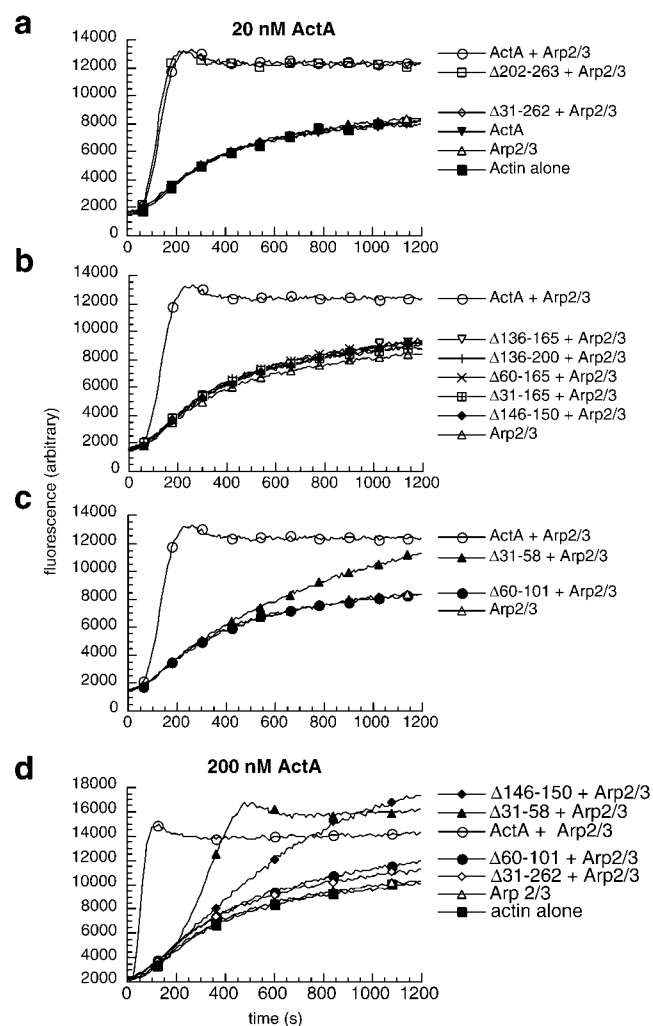
To better assess the contribution of each region within the NH₂-terminal domain of ActA to actin nucleation, we generated and purified a series of 6xHis-tagged in-frame deletion derivatives of ActA (Fig. 3, a and b). The capacity of these derivatives to nucleate polymerization with the Arp2/3 complex was determined using the pyrene-actin polymerization assay. Consistent with the results of the truncation analysis, a derivative lacking the entire NH₂-terminal domain (Δ31-262) was unable to enhance nucleation when present at an equal concentration (Fig. 4 a) or at a 10-fold molar excess (Fig. 4 d) with respect to the Arp2/3 complex. Another derivative (Δ202-263), which based on the truncation analysis was missing amino acids that are not critical for nucleation, was as active as full-length ActA (Fig. 4 a), indicating that large deletions within this domain can be tolerated without reducing activity.

A derivative missing the region that harbors the cofilin homology sequence (Δ136-165) had virtually no stimulatory effect on polymerization kinetics when added at equimolar concentrations with the Arp2/3 complex (Fig. 4 b). Other ActA derivatives containing larger deletions encompassing this region (Δ136-200, Δ60-165, and Δ31-165) exhibited comparable activity at this same concentration (Fig. 4 b). To more specifically assess the function of the cofilin homology sequence, a derivative was constructed in which the five basic residues at the core of this sequence were removed (Δ146-150; Fig. 3 a). The activity of this pro-



*Figure 3.* In-frame ActA deletions. (a) Diagram of secreted 6xHis-tagged derivatives of ActA that contain in-frame deletions within the NH₂-terminal domain. Deleted residues are indicated on the left. (b) Purified derivatives of ActA containing in-frame deletions visualized on a 7.5% polyacrylamide gel stained with Coomassie blue.
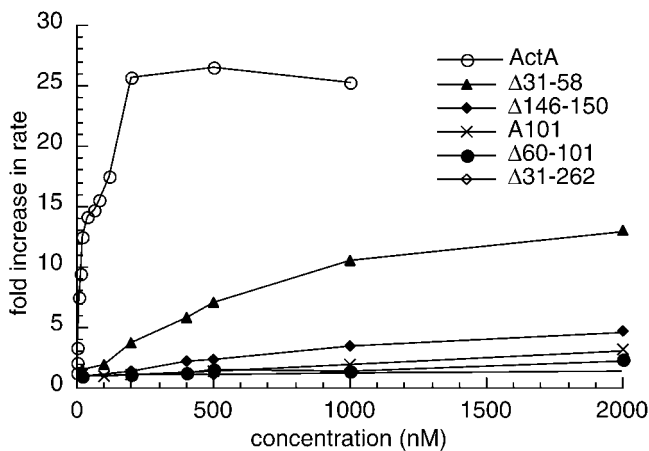


*Figure 4.* Effects of ActA deletion derivatives and the Arp2/3 complex on the kinetics of actin polymerization. (a–d) Graphs of fluorescence intensity versus time after initiating polymerization in the pyrene-actin polymerization assay. (a–c) 2 μM actin in the presence or absence of 20 nM Arp2/3 complex and 20 nM ActA derivatives. (d) 2 μM actin in the presence or absence of 20 nM Arp2/3 complex and 200 nM ActA derivatives.

tein was identical to those with larger deletions encompassing this region (Fig. 4 b). Because of the relatively conservative nature of its lesion, Δ146-150 was chosen for further analysis. Increasing the concentration of Δ146-150 to 10-fold molar excess over the Arp2/3 complex resulted in an increase in its nucleating activity relative to lower concentrations (Fig. 4 d), although the degree of stimulation was far less than that of the full-length protein. This indicates that Δ146-150 retains some concentration-dependent nucleating activity.

An ActA derivative harboring a deletion of the acidic stretch (Δ31-58) was able to accelerate nucleation when added at equal concentrations relative to the Arp2/3 complex, but was less active than full-length ActA (Fig. 4 c). Increasing the concentration of Δ31-58 to a 10-fold excess over the Arp2/3 complex resulted in a higher degree of stimulation (Fig. 4 d). At both the lower and higher concentrations, Δ31-58 was less potent than the full-length protein, but more potent than mutants lacking the cofilin homology sequence. Finally, a derivative missing the putative actin-binding region (Δ60-101; Lasa et al., 1997; Cicchetti et al., 1999) caused virtually no enhancement of polymerization kinetics when combined at equal concentrations (Fig. 4 c) or a 10-fold excess relative to the Arp2/3 complex (Fig. 4 d). At both concentrations, the activity of Δ60-101 was comparable to that of Δ31-262 (Fig. 4, c and d), which is missing the entire NH$_2$-terminal domain and is essentially inactive.

The relative activities of the derivatives missing the cofilin homology sequence (Δ146-150), the putative actin-binding region (Δ60-101), and the acidic stretch (Δ31-58) were quantified and compared. For increasing concentrations of each derivative, the fold stimulation of the maximum rate of polymerization with the Arp2/3 complex was plotted versus the concentration of the derivative (Fig. 5). Full-length ActA stimulated the maximal rate of polymerization up to 25-fold, reaching saturation at a concentration

10 times that of the Arp2/3 complex. In contrast, at concentrations 100 times that of Arp2/3 complex, Δ146-150 stimulated polymerization 5-fold (1/5 of the maximum achieved by full-length), Δ60-101 stimulated polymerization 2-fold (1/12 that of full-length), and Δ31-58 stimulated polymerization 13-fold (1/2 that of full-length). Thus, the cofilin homology sequence and the acidic stretch are important for stimulating nucleation, and the putative actin-binding region plays an essential role in this process in vitro.

## ActA Binds Actin Monomer through Its Actin-binding Region

To confirm that ActA binds to actin monomer (Lasa et al., 1997; Cicchetti et al., 1999), and to assess the location of the actin-binding region, we evaluated the ability of the full-length ActA and selected truncation and deletion derivatives to inhibit the rate of actin polymerization (Fig. 6 a). Increasing concentrations of the full-length ActA in-
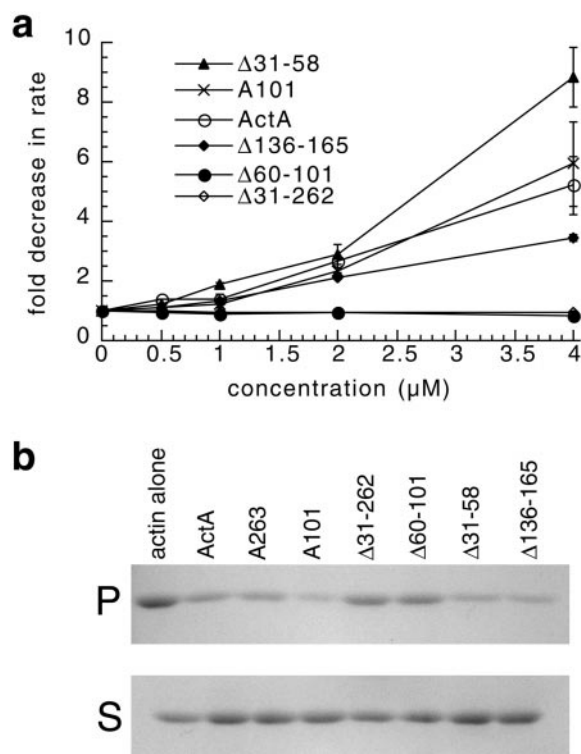
*Figure 6.* High concentrations of ActA and a subset of ActA derivatives slow actin polymerization in the absence of the Arp2/3 complex. (a) Graph of the fold inhibition of the maximal rate of pyrene-actin polymerization versus the concentration of ActA or ActA derivatives. The pyrene-actin assay was carried out in the presence of 2 μM actin and the indicated concentrations of ActA derivatives. The fold inhibition was calculated by dividing the maximal rate of polymerization of actin alone by the maximal rate of polymerization in the presence of ActA (bars represent SEM). (b) An actin pelleting assay was used to assess the inhibitory effect of ActA and ActA derivatives on actin polymerization. 1 μM actin was polymerized for 10 min in the presence or absence of 5 μM ActA or ActA derivatives. Actin filaments (F-actin) were separated from monomers (G-actin) by centrifugation. The amount of F-actin in the pellet (P) and G-actin in the supernatant (S) fractions was visualized on a 12% polyacrylamide gel stained with Coomassie blue.

*Figure 5.* Graph of the fold increase in the maximal rate of pyrene-actin polymerization versus the concentration of ActA or ActA derivatives. Pyrene-actin assays were carried out in the presence of 2 μM actin, 20 nM Arp2/3 complex, and the indicated concentrations of ActA or its derivatives. The fold increase in the rate of polymerization was calculated by dividing the maximum rate of polymerization in the presence of the Arp2/3 complex and ActA or ActA derivatives by the maximum rate of polymerization in the presence of the Arp2/3 complex alone.

cluded in the pyrene-actin assay (in the absence of the Arp2/3 complex) caused a dose-dependent reduction in the maximum rate of polymerization (Fig. 6 a), but did not affect the steady state amount of actin polymer (not shown). Deletion of the $NH_2$-terminal domain of ActA ($\Delta$31-262) or the putative actin-binding region ($\Delta$60-101) rendered ActA unable to inhibit actin polymerization even at a two-fold molar excess relative to actin. In contrast, a truncation derivative consisting of the acidic and actin-binding regions (A101) and the deletion derivatives, missing the acidic stretch ($\Delta$31-58) and the cofilin homology region ($\Delta$136-165), was still able to inhibit actin polymerization. Deletion of the acidic stretch slightly enhanced the ability of ActA to inhibit actin polymerization, whereas deletion of the cofilin homology sequence slightly retarded this activity. The inhibition of polymerization was due to actin monomer binding and not filament capping because derivatives did not inhibit filament depolymerization in a pyrene-actin depolymerization assay (data not shown). These results were confirmed by measuring the ability of ActA derivatives to inhibit polymerization when included at a five-fold molar excess relative to actin in a pelleting assay (Fig. 6 b). Our results demonstrate that ActA binds to the actin monomer through an actin-binding region located between amino acids 60 and 101. Taken together with the activity of $\Delta$60-101 in the presence of the Arp2/3 complex, these data indicate that actin monomer binding is critical for stimulating actin nucleation with the Arp2/3 complex in vitro.

### ActA Binds Directly to the Arp2/3 Complex

Although ActA functions with the Arp2/3 complex in actin nucleation, no direct binding interaction between these two factors has yet been demonstrated. To test for a direct interaction, Arp2/3 complex was bound to protein A beads via an antibody to the p41 subunit of the complex. ActA or its deletion derivatives were tested for their ability to pellet with the Arp2/3 affinity matrix (Fig. 7). Full-length ActA bound to Arp2/3-coated beads, but not to beads coated with nonspecific IgG. In contrast, the $\Delta$31-262 derivative lacking the entire $NH_2$-terminal domain did not bind to the complex, indicating that the $NH_2$-terminal domain is required for this interaction. Derivatives missing the cofilin homology sequence ($\Delta$136-165), the actin-binding region ($\Delta$60-101), and the acidic stretch ($\Delta$31-58) all bound to the Arp2/3 complex. These data suggest that no single region within the $NH_2$-terminal domain is solely responsible for binding to the complex.

### Mutations in ActA that Affect Arp2/3 Complex-mediated Actin Nucleation In Vitro Cause Defects in Actin Polymerization and Actin-based Motility In Vivo

To correlate the effect of deletion mutations on actin nucleation in vitro with their effect on actin-based motility in cells, we replaced the wild-type chromosomal *actA* gene in *L. monocytogenes* with the mutated versions using allelic exchange (Camilli et al., 1993). We confirmed that each mutant protein was expressed on the bacterial surface at levels comparable to wild type by visualizing surface-extracted ActA using SDS-PAGE and Western blotting
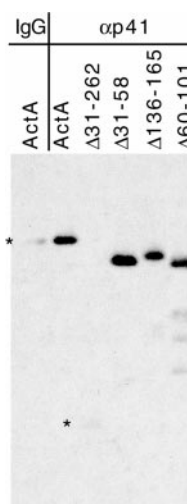


*Figure 7.* Binding of ActA and ActA derivatives to Arp2/3 complex–coated resin. Equimolar concentrations of ActA or the indicated ActA derivatives were incubated with anti-p41-Arp2/3–coated resin or control IgG–coated resin. Bound ActA and ActA derivatives were resolved on a 7% polyacrylamide gel and visualized by Western blotting with polyclonal anti-ActA antibody. The expected mobility of ActA and $\Delta$31-262 is indicated by a star.

(Fig. 8). Each mutant strain was used to infect both HeLa and PtK2 cells, and its capacity to associate with F-actin (filamentous actin) and to undergo actin-based motility was observed and quantified (Fig. 9 a and Table II). To confirm that ActA derivatives were properly expressed in host cytoplasm, infected HeLa cells were subjected to immunofluorescence using antibody raised against human VASP, a cellular protein that binds to ActA's proline-rich repeats (Pistor et al., 1995). VASP colocalized with all strains expressing ActA derivatives containing the proline-rich region (Fig. 9 b, not shown), indicating that ActA was expressed on the bacterial surface. All other quantification was carried out in PtK2 cells, whose flat morphology facilitates counting bacteria that are not well separated (Fig. 9 a and Table II; similar results were obtained in HeLa cells, Fig. 9 b).

At 3.5 h after infection, nearly all (99%) of wild-type *L. monocytogenes* were able to polymerize F-actin and the majority (51%) were motile, based on their association with actin comet tails (Theriot et al., 1992). In contrast, none of the mutants carrying deletions of the cofilin homology sequence ($\Delta$7-632, $\Delta$31-165, $\Delta$136-200, $\Delta$60-165, and $\Delta$146-150) were motile or capable of polymerizing actin in these cell types, leading to the accumulation of microcolonies near the center of the cell. Intermediate phenotypes were exhibited by mutants missing the acidic domain ($\Delta$31-58; 73% F-actin positive; 12% with tails), the actin-binding re-
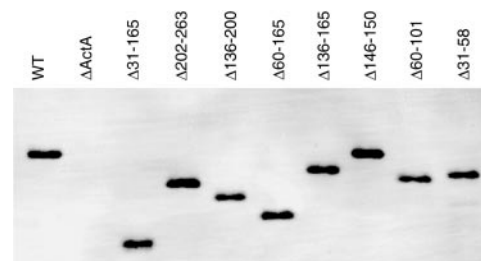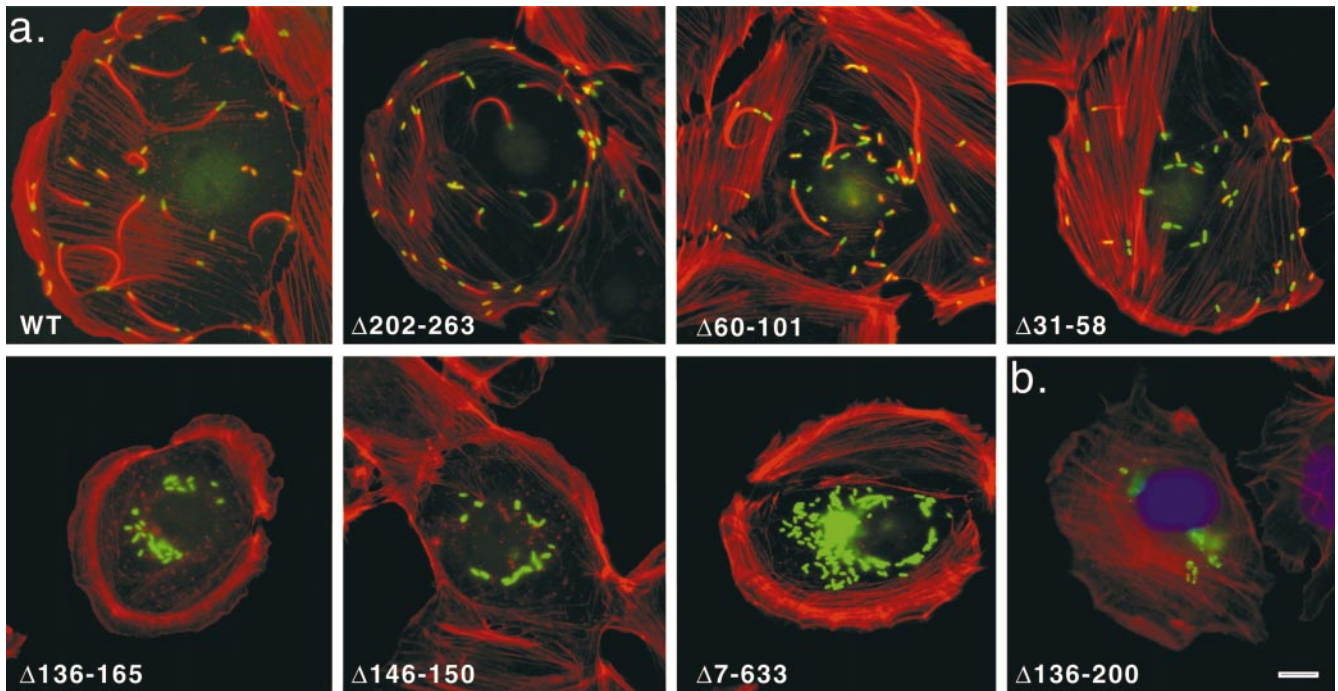


*Figure 8.* Surface-associated ActA from *actA* mutants visualized by Western blotting. Surface proteins were extracted from an equivalent number of bacteria and separated on a 7% polyacrylamide gel. ActA was detected by Western blotting using polyclonal anti-ActA antibody.

*Figure 9.* Actin and *L. monocytogenes* visualized in infected PtK2 and HeLa cells. (a) PtK2 cells infected for 3.5 h with wild-type *L. monocytogenes* or the indicated mutants expressing surface-associated deletion derivatives of ActA. F-actin was visualized by staining with rhodamine-conjugated phalloidin, and bacteria were detected by indirect immunofluorescence using polyclonal anti-*L. monocytogenes* primary antibody followed by FITC-conjugated secondary antibody. (b) HeLa cells infected with Δ136-200 mutant *L. monocytogenes* for 3.5 h. F-actin was stained with rhodamine-phalloidin, DNA with DAPI, and VASP with polyclonal anti-VASP primary antibody followed by FITC-conjugated secondary antibody. Bars, 10 μm.

gion (Δ60-101; 75% F-actin positive; 30% with tails), or the region COOH-terminal to the cofilin homology sequence (Δ202-263; 99% F-actin positive; 28% with tails). These data suggest that the cofilin homology sequence is essential for actin polymerization in cells, whereas the other regions contribute to both actin polymerization and motility.

For those mutant strains that formed actin comet tails in infected PtK2 cells, rates of intracellular motility were determined using time-lapse phase microscopy (Table II). Compared with wild-type *L. monocytogenes*, Δ202-263 (4% reduced), Δ60-101 (18% reduced), and Δ31-58 (34% reduced) mutants exhibited similar or moderately lower mean motility rates. These results suggest that once bacteria are able to initiate actin polymerization, deletions within the NH₂-terminal region of ActA cause only small changes in the velocity of movement.

### actA Alleles Affect the Ability of L. monocytogenes to Spread from Cell to Cell

To correlate the effects of *actA* mutations on actin-based motility with their effects on *L. monocytogenes* cell-to-cell spread, mutant strains were tested for their ability to form a plaque in a monolayer of mouse L2 fibroblast cells (Table II). Wild-type *L. monocytogenes* (defined as 100% plaque size) and the Δ202-263 mutant formed nearly equivalent-sized plaques. Mutants that expressed derivatives lacking the cofilin homology sequence (Δ7-633, Δ31-165, Δ136-200, Δ60-165, Δ136-165, and Δ146-150), which were unable to polymerize actin in cells, were unable to form plaques. Mutants lacking the actin-binding region

(Δ60-101) or the acidic stretch (Δ31-58) exhibited a reduced mean plaque size. Thus, there is a good correlation between the capacity of the mutants to undergo actin-based motility and their ability to spread from cell to cell.

## Discussion

Actin nucleation at the *L. monocytogenes* surface is mediated by the host Arp2/3 complex together with the NH₂-terminal domain of the bacterial ActA protein. Although extensive analysis of the function of the NH₂-terminal domain has been conducted (Pistor et al., 1995; Lasa et al., 1997; Mourrain et al., 1997), the regions within this domain that stimulate nucleation with the Arp2/3 complex have not been identified, and their corresponding contribution to actin-based motility and pathogenesis in cells has not been determined. Through systematic truncation and deletion mutagenesis, we provide evidence that three regions in ActA play important roles in stimulating actin nucleation with the Arp2/3 complex in vitro, and that these regions share similarities with eukaryotic WASP family proteins. Examination of the phenotypes exhibited by mutant *L. monocytogenes* in infected cells indicates that each region performs a distinct function in actin-based motility, and that a single region centered around the cofilin homology sequence is essential for motility and pathogenesis.

### ActA Mimics WASP Family Proteins

*L. monocytogenes* capitalizes on a host mechanism of actin-based motility to spread from cell to cell, perhaps by

Table II. Intracellular Phenotypes of L. monocytogenes Expressing Different actA Alleles

| actA allele | Plaque size | | | | | | F-actin association | | |
| | Diameter percent WT | SD | n* | Intracellular motility | | | Percent F-actin positive | Percent actin tails | n* |
| | | | | Mean rate | SEM | n* | | | |
| --- | --- | --- | --- | --- | --- | --- | --- | --- | --- |
| | | | | *μm/min* | | | | | |
| WT | 100 | na | 9 | 9.8 | 0.6 | 41 | 99 | 51 | 952 |
| D202-263 | 95 | 2.3 | 9 | 9.4 | 0.7 | 50 | 99 | 28 | 867 |
| Δ31-58 | 48 | 4.6 | 9 | 6.5 | 0.4 | 54 | 73 | 12 | 987 |
| Δ60-101 | 59 | 2.2 | 9 | 8 | 0.5 | 48 | 75 | 30 | 1,195 |
| Δ146-150 | 0 | 0 | 9 | | | | 0 | 0 | 660 |
| Δ136-165 | 0 | 0 | 8 | | | | 0 | 0 | 473 |
| Δ136-200 | 0 | 0 | 8 | | | | 0 | 0 | 654 |
| Δ60-165 | 0 | 0 | 8 | | | | 0 | 0 | 501 |
| Δ31-165 | 0 | 0 | 8 | | | | 0 | 0 | 342 |
| Δ7-633 | 0 | 0 | 8 | | | | 0 | 0 | 751 |

*For plaque size, *n* equals number of independent experiments, whereas for intracellular motility rates and F-actin association, *n* equals total number of bacteria counted.

mimicking the function of endogenous proteins that promote actin nucleation. One such class of host factors is the WASP family of proteins (including WASP, N-WASP, Las17p/Bee1p, and Scar/WAVE), which stimulate actin nucleation with the Arp2/3 complex in vitro (Egile et al., 1999; Machesky et al., 1999; Rohatgi et al., 1999; Winter et al., 1999; Yarar et al., 1999) and direct actin-based motility in cell cytoplasm (Suzuki et al., 1998; Egile et al., 1999; Yarar et al., 1999). We found that the minimal fragment of ActA that retains full activity in vitro can be divided into three regions, which have counterparts in the minimal active fragment of WASP family proteins (Higgs et al., 1999; Machesky et al., 1999; Rohatgi et al., 1999; Winter et al., 1999). These include an acidic stretch and a cofilin homology sequence that share limited sequence similarity with corresponding regions in WASP family proteins (Bi and Zigmond, 1999), as well as an actin monomer–binding region that is not similar in sequence to the monomer-binding WH2 (WASP homology 2 or Verprolin homology) domain of WASP proteins. This correspondence suggests that ActA and WASP family proteins function by similar mechanisms.

### The Cofilin Homology Sequence Is Critical for Actin Nucleation In Vitro and in Cells

An ActA derivative lacking only five amino acids at the core of the cofilin homology sequence (Δ146-150) is severely compromised in its capacity to stimulate nucleation with the Arp2/3 complex, but a mutant that lacks this entire region (Δ136-165) can still bind the complex. Similarly, a derivative of N-WASP, lacking the cofilin homology sequence, has a dramatically reduced ability to stimulate actin nucleation (Rohatgi et al., 1999), and exhibits a slightly reduced capacity to bind to the Arp2/3 complex (Banzai et al., 2000). Therefore, this sequence element plays a critical role in stimulating nucleation in both proteins, perhaps by participating in binding to the Arp2/3 complex and/or by inducing a conformational change in the complex that facilitates nucleation.

Consistent with the severe defects exhibited by the Δ146-150 derivative in vitro, L. monocytogenes mutants expressing Δ146-150 on their surface do not associate with actin in HeLa or PtK2 cells and do not form plaques in an L2 cell monolayer. However, a small percentage of L. monocytogenes that express Δ146-150 are capable of associating with actin in MDCK and J774 cells (Lauer, P., J. Theriot, and D. Portnoy, unpublished results). In addition, mutants that overexpress this derivative form actin clouds, but not actin tails, in Xenopus laevis egg extract (Lasa et al., 1997). The discrepancy between the behaviors of this mutant in different cytoplasmic environments may reflect differences in the concentration of host cytoskeletal proteins. Nevertheless, the mutant phenotypes indicate that the cofilin homology sequence is critical for pathogenesis and, while not necessary for actin nucleation, is required to achieve the threshold of activity needed to initiate actin-based motility.

### The Acidic Stretch Plays a Nonessential Role in Nucleation and Intracellular Motility

ActA fragments consisting only of the acidic stretch and actin-binding region possess stimulatory activity, indicating that these elements play a role in nucleation. Moreover, a derivative lacking the acidic stretch (Δ31-58) retains the capacity to bind the Arp2/3 complex and exhibits a modest reduction in maximum activity compared with full-length ActA in vitro. This suggests that the acidic stretch may function with the cofilin homology sequence to promote nucleation by facilitating a productive interaction with the Arp2/3 complex. Interestingly, the acidic stretch in N-WASP is essential for Arp2/3 complex binding and for stimulating nucleation (Rohatgi et al., 1999), suggesting that ActA may exhibit more redundancy in its binding and activation mechanism.

Compared with the wild type, mutants expressing Δ31-58 exhibit a diminished percentage of bacteria that polymerize actin, a reduced percentage of moving bacteria, a reduced mean rate of motility, and an impaired capacity to spread from cell to cell. These phenotypes point to a direct correlation between the nucleation activity of the Arp2/3 complex with ActA in vitro and the efficiency of actin polymerization and L. monocytogenes motility in cells.

### The Actin-binding Region Is Necessary for Nucleation In Vitro but Not in Cells

The results of our study confirm the actin monomer–binding activity of ActA (Lasa et al., 1997; Cicchetti et al., 1999) and extend previous studies by addressing the role of monomer binding in nucleation and motility. An ActA derivative missing the monomer-binding region was virtually unable to stimulate Arp2/3-mediated nucleation in vitro, suggesting that actin binding is critical for nucleation in the context of purified proteins. Similarly, the actin binding WH2 domain of N-WASP is critical for stimulating nucleation (Rohatgi et al., 1999). The essential function of this region may be to position an actin monomer in close proximity to the Arp2/3 complex, forming a trimeric nucleus (Fig. 10) consisting of the two actin-related proteins in the complex and the actin monomer bound to ActA.
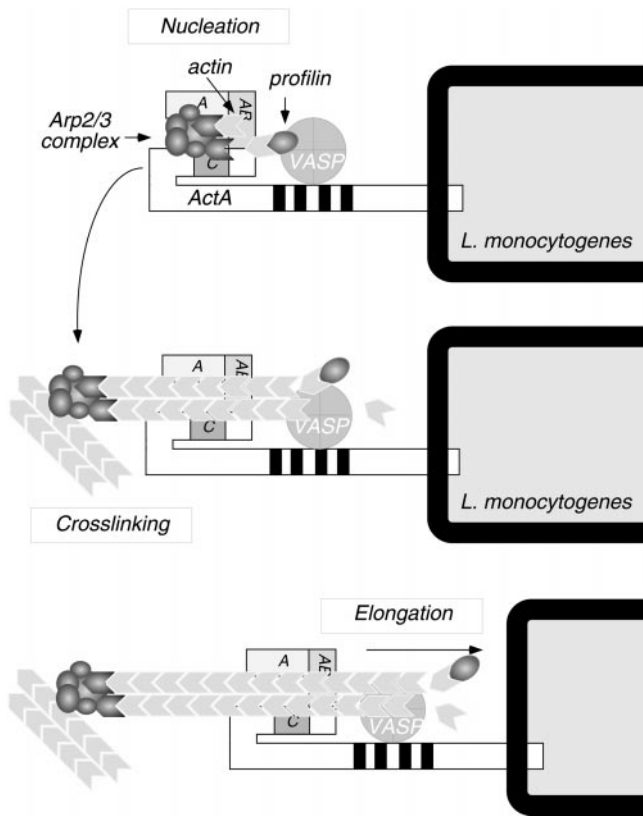
*Figure 10.* Model for actin nucleation by ActA and the Arp2/3 complex at the *L. monocytogenes* surface. The NH$_2$-terminal domain of ActA interacts directly with the Arp2/3 complex. The acidic stretch (A) and cofilin homology sequence (C) of ActA both contribute to Arp2/3 complex activation, whereas the actin-binding region (AB) recruits and presents the actin monomer to facilitate formation of an actin nucleus. After nucleation takes place, the Arp2/3 complex dissociates from ActA, and its cross-linking activity contributes to the structure of the comet tail. During bacterial motility, profilin may speed the rate of filament elongation by delivering actin monomers to the exposed barbed ends of nucleated filaments, and VASP may bind newly formed filaments to help maintain their association with the bacterial surface.

In contrast to the loss of activity in vitro, mutant *L. monocytogenes* expressing the monomer-binding deletion still associate with F-actin, are motile, and can spread from cell to cell, although each of these parameters is slightly impaired compared with the wild type. Thus, actin binding by ActA may serve a redundant function in cells, perhaps because other ActA-associated proteins in host cytosol bind actin monomer in a manner that facilitates nucleation (Fig. 10). One candidate monomer-binding protein is profilin, which localizes to the surface of *L. monocytogenes* (Theriot et al., 1994) through interactions with host Ena/ VASP family proteins (Reinhard et al., 1995; Gertler et al., 1996; Kang et al., 1997) that bind directly to the proline-rich repeats of ActA (Chakraborty et al., 1995; Pistor et al., 1995; Smith et al., 1996; Niebuhr et al., 1997).

### The Role of Actin Nucleation by ActA and the Arp2/3 Complex in L. monocytogenes Motility

We propose a model in which actin nucleation at the *L.*

*monocytogenes* surface results from an interaction between monomeric actin and the Arp2/3 complex with at least three regions within the NH$_2$-terminal domain of ActA (Fig. 10). Interaction of the Arp2/3 complex with the cofilin homology sequence and the acidic stretch may induce a conformational change in the complex that promotes nucleation. Nucleation may also require correct positioning of an actin monomer in close proximity to the Arp2/3 complex, a function provided by the actin-binding region in ActA or, alternatively, by host proteins such as profilin, which are associated with ActA in cell cytoplasm. Bound actin monomer would complete a nucleation site, whose formation would be unfavorable in the absence of ActA, because the Arp2/3 complex alone is thought to nucleate by binding rare and unstable actin dimers (Mullins et al., 1998). Elongation of newly formed filaments at the bacterial surface may be facilitated by profilin and VASP, which enhance bacterial motility in a system of purified proteins (Loisel et al., 1999). The similarities between ActA and WASP family proteins suggest that they represent a fascinating example of convergent evolution. Interestingly, the unrelated bacterial pathogen *Shigella flexneri* initiates actin-based motility by recruiting and activating N-WASP at its surface rather than mimicking its activity (Suzuki et al., 1998; Egile et al., 1999). Further understanding of the mechanism of ActA-Arp2/3–mediated actin nucleation will lead us to a greater understanding of cell motility and the mechanisms of microbial pathogenesis.

### References

Banzai, Y., H. Miki, H. Yamaguchi, and T. Takenawa. 2000. Essential role of neural Wiskott-Aldrich syndrome protein in neurite extension in PC12 cells and rat hippocampal primary culture cells. *J. Biol. Chem.* 275:11987–11992.

Bachmann, C., L. Fischer, U. Walter, and M. Reinhard. 1999. The EVH2 domain of the vasodilator-stimulated phosphoprotein mediates tetramerization, F-actin binding, and actin bundle formation. *J. Biol. Chem.* 274:23549–23557.

Bi, E., and S.H. Zigmond. 1999. Actin polymerization: where the WASP stings. *Curr. Biol.* 9:R160–R163.

Brundage, R.A., G.A. Smith, A. Camilli, J.A. Theriot, and D.A. Portnoy. 1993. Expression and phosphorylation of the *Listeria monocytogenes* ActA protein in mammalian cells. *Proc. Natl. Acad. Sci. USA.* 90:11890–11894.

Cameron, L.A., M.J. Footer, A. van Oudenaarden, and J.A. Theriot. 1999. Motility of ActA protein-coated microspheres driven by actin polymerization. *Proc. Natl. Acad. Sci. USA.* 96:4908–4913.

Camilli, A., L.G. Tilney, and D.A. Portnoy. 1993. Dual roles of *plcA* in *Listeria monocytogenes* pathogenesis. *Mol. Microbiol.* 8:143–157.

Chakraborty, T., F. Ebel, E. Domann, K. Niebuhr, B. Gerstel, S. Pistor, C.J. Temm-Grove, B.M. Jockusch, M. Reinhard, U. Walter, et al. 1995. A focal adhesion factor directly linking intracellularly motile *Listeria monocytogenes* and *Listeria ivanovii* to the actin-based cytoskeleton of mammalian cells. *EMBO (Eur. Mol. Biol. Organ.) J.* 14:1314–1321.

Chou, P.Y., and G.D. Fasman. 1974. Prediction of protein conformation. *Biochemistry.* 13:222–245.

Cicchetti, G., P. Maurer, P. Wagener, and C. Kocks. 1999. Actin and phosphoinositide binding by the ActA protein of the bacterial pathogen *Listeria monocytogenes. J. Biol. Chem.* 274:33616–33626.

Cooper, J.A., S.B. Walker, and T.D. Pollard. 1983. Pyrene actin: documentation of the validity of a sensitive assay for actin polymerization. *J. Muscle Res. Cell Motil.* 4:253–262.

Domann, E., J. Wehland, M. Rohde, S. Pistor, M. Hartl, W. Goebel, M. Leimeister-Wachter, M. Wuenscher, and T. Chakraborty. 1992. A novel bacterial virulence gene in *Listeria monocytogenes* required for host cell microfilament interaction with homology to the proline-rich region of vinculin. *EMBO (Eur. Mol. Biol. Organ.) J.* 11:1981–1990.

Egile, C., T.P. Loisel, V. Laurent, R. Li, D. Pantaloni, P.J. Sansonetti, and M.F. Carlier. 1999. Activation of the CDC42 effector N-WASP by the *Shigella flexneri* IcsA protein promotes actin nucleation by Arp2/3 complex and bacterial actin-based motility. *J. Cell Biol.* 146:1319–1332.

Gertler, F.B., K. Niebuhr, M. Reinhard, J. Wehland, and P. Soriano. 1996. Mena, a relative of VASP and *Drosophila* Enabled, is implicated in the control of microfilament dynamics. *Cell.* 87:227–239.

Higgs, H.N., L. Blanchoin, and T.D. Pollard. 1999. Influence of the C terminus of Wiskott-Aldrich Syndrome protein (WASp) and the Arp2/3 complex on actin polymerization. *Biochemistry.* 38:15212–15222.

Horton, R.M., Z. Cai, S.N. Ho, and L.R. Pease. 1990. Gene splicing by overlap extension: tailor-made genes using the polymerase chain reaction. *Biotechniques.* 8:528–535.

Ireton, K., and P. Cossart. 1997. Host-pathogen interactions during entry and actin-based movement of *Listeria monocytogenes. Annu. Rev. Genet.* 31: 113–138.

Jones, S., and D.A. Portnoy. 1994. Small plaque mutants. *Methods Enzymol.* 236:526–531.

Kang, F., R.O. Laine, M.R. Bubb, F.S. Southwick, and D.L. Purich. 1997. Profilin interacts with the Gly-Pro-Pro-Pro-Pro-Pro sequences of vasodilator-stimulated phosphoprotein VASP: implications for actin-based *Listeria* motility. *Biochemistry.* 36:8384–8392.

Kocks, C., E. Gouin, M. Tabouret, P. Berche, H. Ohayon, and P. Cossart. 1992. *L. monocytogenes*-induced actin assembly requires the actA gene product, a surface protein. *Cell.* 68:521–531.

Kouyama, T., and K. Mihashi. 1981. Fluorimetry study of N-(1-pyrenyl)iodoacetamide-labelled F-actin. Local structural change of actin protomer both on polymerization and on binding of heavy meromyosin. *Eur. J. Biochem.* 114:33–38.

Lasa, I., V. David, E. Gouin, J.B. Marchand, and P. Cossart. 1995. The aminoterminal part of ActA is critical for the actin-based motility of *Listeria monocytogenes*; the central proline-rich region acts as a stimulator. *Mol. Microbiol.* 18:425–436.

Lasa, I., E. Gouin, M. Goethals, K. Vancompernolle, V. David, J. Vandekerckhove, and P. Cossart. 1997. Identification of two regions in the N-terminal domain of ActA involved in the actin comet tail formation by *Listeria monocytogenes. EMBO (Eur. Mol. Biol. Organ.) J.* 16:1531–1540.

Loisel, T.P., R. Boujemaa, D. Pantaloni, and M.F. Carlier. 1999. Reconstitution of actin-based motility of Listeria and Shigella using pure proteins. *Nature.* 401:613–616.

Machesky, L.M., and K.L. Gould. 1999. The Arp2/3 complex: a multifunctional actin organizer. *Curr. Opin. Cell Biol.* 11:117–121.

Machesky, L.M., and R.H. Insall. 1999. Signaling to actin dynamics. *J. Cell Biol.* 146:267–272.

Machesky, L.M., R.D. Mullins, H.N. Higgs, D.A. Kaiser, L. Blanchoin, R.C. May, M.E. Hall, and T.D. Pollard. 1999. Scar, a WASp-related protein, activates nucleation of actin filaments by the Arp2/3 complex. *Proc. Natl. Acad. Sci. USA.* 96:3739–3744.

May, R.C., M.E. Hall, H.N. Higgs, T.D. Pollard, T. Chakraborty, J. Wehland, L.M. Machesky, and A.S. Sechi. 1999. The Arp2/3 complex is essential for the actin-based motility of *Listeria monocytogenes. Curr. Biol.* 9:759–762.

Mogilner, A., and G. Oster. 1996. Cell motility driven by actin polymerization. *Biophys. J.* 71:3030–3045.

Moors, M.A., V. Auerbuch, and D.A. Portnoy. 1999. Stability of the *Listeria monocytogenes* ActA protein in mammalian cells is regulated by the N-end rule pathway. *Cell. Microbiol.* 1:249–258.

Mourrain, P., I. Lasa, A. Gautreau, E. Gouin, A. Pugsley, and P. Cossart. 1997. ActA is a dimer. *Proc. Natl. Acad. Sci. USA.* 94:10034–10039.

Mullins, R.D., W.F. Stafford, and T.D. Pollard. 1997. Structure, subunit topology, and actin-binding activity of the Arp2/3 complex from *Acanthamoeba. J. Cell Biol.* 136:331–343.

Mullins, R.D., J.A. Heuser, and T.D. Pollard. 1998. The interaction of Arp2/3 complex with actin: nucleation, high affinity pointed end capping, and formation of branching networks of filaments. *Proc. Natl. Acad. Sci.* 95:6181–6186.

Niebuhr, K., F. Ebel, R. Frank, M. Reinhard, E. Domann, U.D. Carl, U. Walter, F.B. Gertler, J. Wehland, and T. Chakraborty. 1997. A novel proline-rich motif present in ActA of *Listeria monocytogenes* and cytoskeletal proteins is the ligand for the EVH1 domain, a protein module present in the Ena/VASP family. *EMBO (Eur. Mol. Biol. Organ.) J.* 16:5433–5444.

Pistor, S., T. Chakraborty, K. Niebuhr, E. Domann, and J. Wehland. 1994. The ActA protein of *Listeria monocytogenes* acts as a nucleator inducing reorganization of the actin cytoskeleton. *EMBO (Eur. Mol. Biol. Organ.) J.* 13: 758–763.

Pistor, S., T. Chakraborty, U. Walter, and J. Wehland. 1995. The bacterial actin nucleator protein ActA of *Listeria monocytogenes* contains multiple binding sites for host microfilament proteins. *Curr. Biol.* 5:517–525.

Reinhard, M., M. Halbrugge, U. Scheer, C. Wiegand, B.M. Jockusch, and U. Walter. 1992. The 46/50 kDa phosphoprotein VASP purified from human platelets is a novel protein associated with actin filaments and focal contacts. *EMBO (Eur. Mol. Biol. Organ.) J.* 11:2063–2070.

Reinhard, M., K. Giehl, K. Abel, C. Haffner, T. Jarchau, V. Hoppe, B.M. Jockusch, and U. Walter. 1995. The proline-rich focal adhesion and microfilament protein VASP is a ligand for profilins. *EMBO (Eur. Mol. Biol. Organ.) J.* 14:1583–1589.

Robbins, J.R., A.I. Barth, H. Marquis, E.L. de Hostos, W.J. Nelson, and J.A. Theriot. 1999. *Listeria monocytogenes* exploits normal host cell processes to spread from cell to cell. *J. Cell Biol.* 146:1333–1350.

Rohatgi, R., L. Ma, H. Miki, M. Lopez, T. Kirchhausen, T. Takenawa, and M.W. Kirschner. 1999. The interaction between N-WASP and the Arp2/3 complex links Cdc42-dependent signals to actin assembly. *Cell.* 97:221–231.

Sanger, J.M., J.W. Sanger, and F.S. Southwick. 1992. Host cell actin assembly is necessary and likely to provide the propulsive force for intracellular movement of *Listeria monocytogenes. Infect. Immun.* 60:3609–3619.

Smith, G.A., D.A. Portnoy, and J.A. Theriot. 1995. Asymmetric distribution of the *Listeria monocytogenes* ActA protein is required and sufficient to direct actin-based motility. *Mol. Microbiol.* 17:945–951.

Smith, G.A., J.A. Theriot, and D.A. Portnoy. 1996. The tandem repeat domain in the *Listeria monocytogenes* ActA protein controls the rate of actin-based motility, the percentage of moving bacteria, and the localization of vasodilator-stimulated phosphoprotein and profilin. *J. Cell Biol.* 135:647–660.

Smith, K., and P. Youngman. 1992. Use of a new integrational vector to investigate compartment-specific expression of the *Bacillus subtilis spoIIM* gene. *Biochimie.* 74:705–711.

Spudich, J.A., and S. Watt. 1971. The regulation of rabbit skeletal muscle contraction. I. Biochemical studies of the interaction of the tropomyosin-troponin complex with actin and the proteolytic fragments of myosin. *J. Biol. Chem.* 246:4866–4871.

Sun, A.N., A. Camilli, and D.A. Portnoy. 1990. Isolation of *Listeria monocytogenes* small-plaque mutants defective for intracellular growth and cell-to-cell spread. *Infect. Immun.* 58:3770–3778.

Suzuki, T., H. Miki, T. Takenawa, and C. Sasakawa. 1998. Neural Wiskott-Aldrich syndrome protein is implicated in the actin-based motility of *Shigella flexneri. EMBO (Eur. Mol. Biol. Organ.) J.* 17:2767–2776.

Theriot, J.A., T.J. Mitchison, L.G. Tilney, and D.A. Portnoy. 1992. The rate of actin-based motility of intracellular *Listeria monocytogenes* equals the rate of actin polymerization. *Nature.* 357:257–260.

Theriot, J.A., J. Rosenblatt, D.A. Portnoy, P.J. Goldschmidt-Clermont, and T.J. Mitchison. 1994. Involvement of profilin in the actin-based motility of *L. monocytogenes* in cells and in cell-free extracts. *Cell.* 76:505–517.

Tilney, L.G., and D.A. Portnoy. 1989. Actin filaments and the growth, movement, and spread of the intracellular bacterial parasite, *Listeria monocytogenes. J. Cell Biol.* 109:1597–1608.

Welch, M.D. 1999. The world according to Arp: regulation of actin nucleation by the Arp2/3 complex. *Trends Cell Biol.* 9:423–427.

Welch, M.D., and T.J. Mitchison. 1998. Purification and assay of the platelet Arp2/3 complex. *Methods Enzymol.* 298:52–61.

Welch, M.D., A. Iwamatsu, and T.J. Mitchison. 1997. Actin polymerization is induced by Arp2/3 protein complex at the surface of *Listeria monocytogenes. Nature.* 385:265–269.

Welch, M.D., J. Rosenblatt, J. Skoble, D.A. Portnoy, and T.J. Mitchison. 1998. Interaction of human Arp2/3 complex and the *Listeria monocytogenes* ActA protein in actin filament nucleation. *Science.* 281:105–108.

Winter, D., T. Lechler, and R. Li. 1999. Activation of the yeast Arp2/3 complex by Bee1p, a WASP-family protein. *Curr. Biol.* 9:501–504.

Wirth, R., F.Y. An, and D.B. Clewell. 1986. Highly efficient protoplast transformation system for *Streptococcus faecalis* and a new *Escherichia coli-S. faecalis* shuttle vector. *J. Bacteriol.* 165:831–836.

Yarar, D., W. To, A. Abo, and M.D. Welch. 1999. The Wiskott-Aldrich syndrome protein directs actin-based motility by stimulating actin nucleation with the Arp2/3 complex. *Curr. Biol.* 9:555–558.